ACS APPLIED MATERIALS & INTERFACES

Research Article

www.acsami.org

Liquid Crystal Droplet-Embedded Biopolymer Hydrogel Sheets for Biosensor Applications

Jinan Deng, Wenlang Liang, and Jiyu Fang*

Advanced Materials Processing and Analysis Center, Department of Materials Science and Engineering, University of Central Florida, Orlando, Florida 32816, United States

ABSTRACT: The development of simple, portable, and low-cost biosensing platforms is of great interest in the clinical diagnosis of disease. Here, we report liquid crystal (LC) droplet-embedded chitosan (CHI) hydrogel films formed by the Ag^+ ion-triggered fast gelation of the CHI/surfactant complex-stabilized LC emulsion which is cast on substrates. The small sheets cut from the LC droplet-embedded hydrogel films combine the advantages of both hydrogels and LC droplets, offering a portable and label-free sensing platform for the real-time detection of bile acids in a small amount of solution. We find that the response time and detection limit of LC droplet-embedded hydrogel sheets for bile acids depend on their chemical structures.

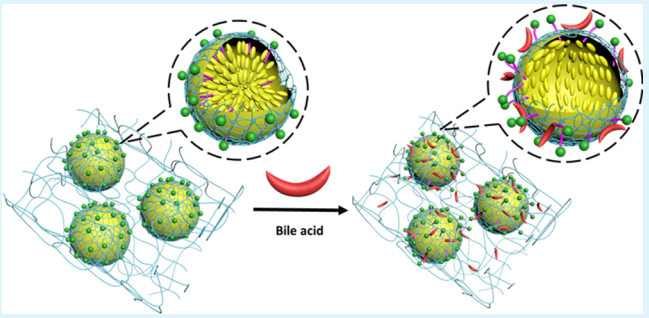

KEYWORDS: *liquid crystals, biopolymers, hydrogel sheets, bile acids, sensors*

1. INTRODUCTION

Liquid crystal (LC) droplets show great potential for biosensor applications because of their large surface area and tunable director configurations.[1,2] It is known that the director configuration of LC droplets is determined by the balance between the surface anchoring energy and the elasticity of the LC inside the droplets.[3] The adsorption and reaction of chemical and biological species at the surface of LC droplets may disturb the balance, consequently inducing the director configuration transition of the LC droplets that can be easily monitored with a polarizing optical microscope.

Recently, polymer-stabilized LC droplets in aqueous solution have been developed as a simple and label-free optical probe for the detection of chemical and biological species.[4−14] For example, Abbott and co-workers reported the use of poly(methacrylic acid)/poly(*N*-vinylpyrrolidone) multilayer-stabilized LC droplets for the detection of lipid-enveloped viruses, in which the lipid transferred from the viruses to the polyelectrolyte multilayer-stabilized LC droplets induced the bipolar-to-radial configuration transition of the LC droplets.[5] Yang and co-workers designed an immune sensor based on polyethylene imine/surfactant complex-coated LC droplets, in which the formation of anti-IgG/IgG complexes at the surface of the LC droplets disrupted the packing of the surfactant and consequently induced the radial-to-bipolar transition of the LC droplets.[7] In a previous publication, we reported the formation of LC droplets in aqueous solution by the adsorption of chitosan (CHI) at the LC−aqueous interface, followed by the penetration of surfactants.[13] The CHI/surfactant complex-coated LC droplets could be used for the detection of bile acids, a biomarker for the clinical diagnosis of liver and intestinal diseases. Although polymer-stabilized LC droplets provide a simple and label-free optical probe, the response time of LC-based sensing platform is largely unknown because the mobility of the LC droplets in aqueous solution limits their applications for the real-time detection of chemical and biological species.

Hydrogels are a cross-linked network structure of hydrophilic polymers. They are able to adsorb a significant amount of water and are highly permeable for biomolecules. Due to their viscoelastic properties, hydrogels can be shaped or cast into different sizes and shapes. These unique features make hydrogels highly desirable for biomedical applications.[15,16] Recent studies have shown that CHI hydrogels can be simply and rapidly fromed from CHI aqueous solution by the complexation of transition metal ions and CHI chains,[17] which provides us a opportunity to integrate LC droplets into CHI hydrogels. In this paper, we report the formation of 4-cyano-4′-pentylbiphenyl (5CB) droplet-embedded CHI hydrogel films by the Ag^+ ion-triggered gelation of CHI/tetradecyl sulfate sodium salt ($SC_{14}S$) complex-stabilized 5CB emulsion cast on substrates, in which the features of both CHI hydrogels and 5CB droplets are synergized. The formation process of the 5CB droplet-embedded CHI hydrogel is shown in Scheme 1. The sheets cut from the 5CB droplet-embedded CHI hydrogel films are used as a portable and label-free sensing platform for the real-time detection of bile acids in a small amount of solution by simply observing the director configuration transition of the embedded 5CB droplets induced by the

Received: November 16, 2015
Accepted: January 22, 2016
Published: January 25, 2016

DOI: 10.1021/acsami.5b11076
ACS Appl. Mater. Interfaces 2016, 8, 3928−3932

Scheme 1. (a) Chemical Structures of 5CB and CHI and (b–e) Schematic Illustrations of the Formation Process of 5CB Droplet-Embedded CHI Hydrogel Films by the Ag^+ Ion-Triggered Fast Gelation of CHI/$SC_{14}S$-Stabilized 5CB Emulsion

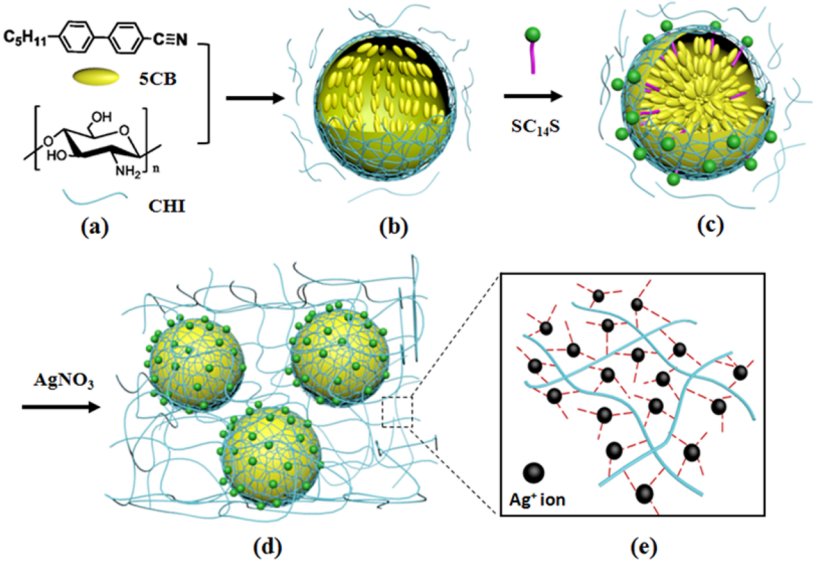

competitive adsorption of the bile acid penetrated through the CHI matrix. The response time and detection limit of the 5CB droplet-embedded hydrogel sheets are found to depend on the hydrophobicity of bile acids.

2. EXPERIMENTAL SECTION

Materials. Chitosan (CHI, low molecular weight), silver nitrate, 4-cyano-4′-pentylbiphenyl (5CB, 98% purity), cholic acid (CA, ≥98% purity), deoxycholic acid (DCA, ≥98% purity), tetradecyl sulfate sodium salt ($SC_{14}S$), and sodium hydroxyl (NaOH) were obtained from Sigma-Aldrich (St. Louis, MO). All chemicals were used without further purification. Water used in our experiments was purified with Easypure II system (18.2 MΩ cm and pH 5.7).

Preparation of CHI/$SC_{14}S$-Stabilized 5CB Droplet Emulsions. A 2 wt % CHI solution was prepared by dissolving CHI in 2% acetic acid solution under magnetic stirring. CHI-stabilized 5CB droplet emulsion was prepared by adding 10 μL of 5CB in 10 mL of 2 wt % CHI aqueous solution at pH 4.05, followed by the tip sonication (FB505, Fisher Scientific, Pittsburgh, PA) at the amplitude of 20% for 10 s at room temperature. The CHI-stabilized 5CB droplets showed a bipolar configuration that transitions to a radial configuration after the addition of 100 μM $SC_{14}S$ in the emulsion.

Preparation of 5CB Droplet-Embedded CHI Hydrogel Films. The formation process of 5CB droplet-embedded CHI hydrogel films is as follows: First, the pH of CHI/$SC_{14}S$ complex-stabilized 5CB emulsion was adjusted to 4.4 by the addition of 0.2 M NaOH. The 80 μL emulsion was then cast on a 18 mm × 18 mm glass substrate. The 5CB droplet-embedded CHI hydrogel film was formed by immersing the cast emulsion in 0.3 M $AgNO_3$ solution for 10 s. The thickness of the resultant CHI hydrogel film was measured to be ∼0.2 mm. The density of CHI/SC14S complex-stabilized 5CB droplets in the emulsion was ∼8.0×10^5 droplets per μL. Therefore, the 5CB droplet density in CHI hydrogel sheets was estimated to be ∼9.9×10^5 droplets per mm^3.

Characterization. The director configuration of 5CB droplets was analyzed with a polarizing optical microscope (Olympus BX40) in transmission mode. The structure of CHI hydrogel films placed on carbon coated grids was characterized with a transmission electron microscope (JEOL TEM-1011, 100 kV). Tensile testing of CHI hydrogel sheets was carried out with a microtensile tester (Tytron 250, MTS Systems Corporation) at room temperature with a loading cell of 5N and a loading speed of 0.1 mm/min. The size of CHI hydrogel sheets for tensile testing was 10 mm × 2 mm.

Detection of Bile Acids with 5CB Droplet-Embedded CHI Hydrogel Sheets. The 5CB-embedded CHI hydrogel film was cut into a small sheet (10 mm length, 2 mm width, and 0.2 mm thickness) that was then placed on the bottom of a small glass dish (MatTek Corporation, MA) with 60 μL of aqueous solution at pH 7.4. The director configuration of the 5CB droplets embedded in CHI hydrogel sheets was in situ monitored with a polarizing optical microscope in transmission mode after the addition of CA and DCA, respectively. The response time was recorded when the 5CB droplets in the focus plane of the microscope over a 50 μm × 50 μm area transitioned into a bipolar configuration for each sheet.

3. RESULTS AND DISCUSSION

Figure 1a shows the polarized optical microscopy image of CHI-stabilized 5CB droplet emulsion, which was formed by adding 10 μL of 5CB in 10 mL of 2 wt % CHI aqueous solution at pH 4.05, followed by sonication. The adsorption of CHI at the 5CB–aqueous interface stabilizes the 5CB droplets in aqueous solution. The CHI-stabilized 5CB droplets show a bipolar configuration, suggesting a parallel surface anchoring of the 5CB inside the droplets (Scheme 1b). After the addition of 100 μM $SC_{14}S$, the director configuration of the CHI-stabilized 5CB droplets becomes radial (Figure 1b), suggesting a perpendicular surface anchoring of the 5CB inside the droplets (Scheme 1c). The bipolar-to-radial configuration transition is a result of the adsorption of $SC_{14}S$ at the surface of CHI-

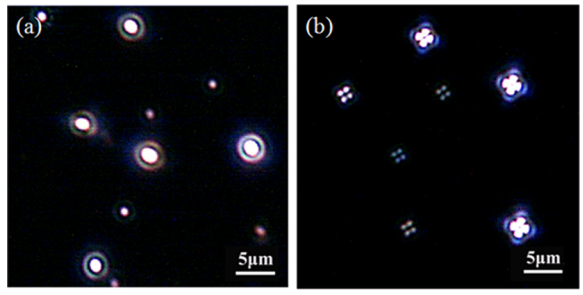

Figure 1. Polarizing optical microscopy images of CHI-stabilized 5CB droplets dispersed in aqueous solution at pH 4.05 (a) before and (b) after the addition of 100 μM $SC_{14}S$.

DOI: 10.1021/acsami.5b11076
ACS Appl. Mater. Interfaces 2016, 8, 3928–3932

stabilized 5CB droplets, in which the negatively charged headgroup of the $SC_{14}S$ is located in the positively charged CHI coating by electrostatic attraction, while the hydrophobic tail of the $SC_{14}S$ extends into the 5CB droplets to induce the radial configuration. In a previous publication, we showed that 5CB droplets could be stabilized in 0.1 wt % CHI aqueous solution.[13] Therefore, there is a large amount of excess CHI in the aqueous phase of the CHI/$SC_{14}S$ complex-stabilized 5CB emulsion formed in 2 wt % CHI aqueous solution. To gel the CHI/$SC_{14}S$ complex-stabilized 5CB emulsion, we first adjusted the pH of the emulsion to 4.4 by the addition of 0.2 M NaOH. The viscous emulsion was then cast on a glass substrate for forming a emulsion film, followed by being immersed in 0.3 M $AgNO_3$ solution for 10 s, in which Ag^+ ions complex with the NH_2 and OH groups of the CHI in the aqueous phase and at the surface of the 5CB droplets, leading to the formation of a 5CB droplet-embedded CHI hydrogel film (Scheme 1d).

The 5CB droplet-embedded hydrogel film can be peeled off from the glass substrate (Figure 2a). The embedded 5CB droplets remain in a radial director configuration in the CHI hydrogel film (Figure 2b), suggesting that the fast gelation process does not change the orientation of the 5CB inside the droplets. Transmission electron microscopy measurements show that the CHI hydrogel film consists of the network of CHI nanofibers with an average diameter of 23.7 ± 6.4 nm (Figure 2c), which are cross-linked by Ag^+ ions through complexing with the NH_2 and OH groups of CHI chains (Scheme 1e). The 5CB droplet-embedded hydrogel films can be cut into sheets (see the inset in Figure 2d). The mechanical properties of the 5CB droplet-embedded hydrogel sheets were studied with tensile testing which was conducted in room temperature at the constant loading speed of 0.1 mm/min. Figure 2d shows a representative strength–strain curve of the 5CB droplet-embedded hydrogel sheets. The tensile strength of the 5CB droplet-embedded hydrogel sheets is 125 kPa with the ultimate strain of ~95%. The extensibility of CHI hydrogel sheets is higher than that of collagen hydrogels (~80%).[18] The Young's modulus of CHI hydrogel sheets is ~63.92 kPa, which is higher than that of collage hydrogels (20 kPa).[19]

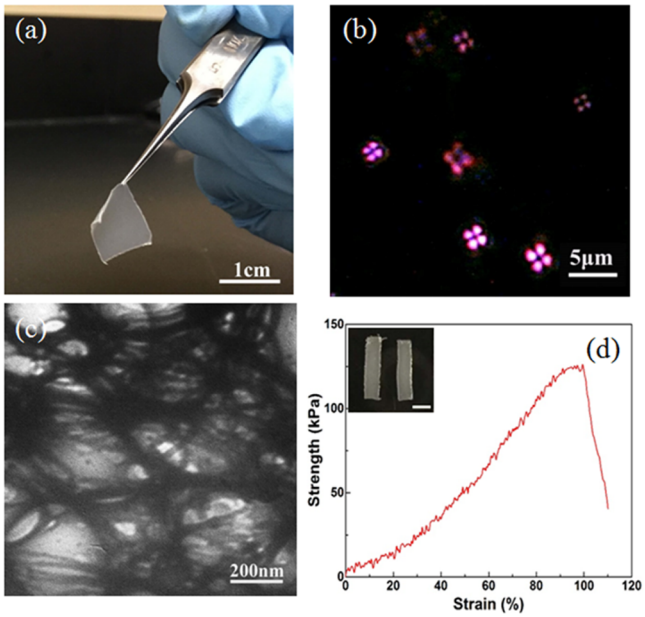

Figure 2. (a) Photography, (b) polarized optical microscopy, and (c) TEM images of 5CB droplet-embedded CHI hydrogel films. (d) Strength–stain curve of 5CB droplet-embedded CHI hydrogel sheets. The photography image of the hydrogel sheets cut from the hydrogel films was inset in part d. The scale bar shown in the inset image is 300 mm.

The good mechanical properties of 5CB droplet-embedded hydrogel sheets make them a suitable sensing platform for the real-time detection of bile acids, in which the competitive adsorption of the bile acid that penetrated through the CHI matrix induces the director configuration transition of the embedded 5CB droplets. Cholic acid (CA) is a primary bile acid which is synthesized from the enzymatic catabolism of cholesterol in the liver.[20] After being secreted into the gut, some of the CAs are dehydroxylated by intestinal bacteria to form deoxycholic acid (DCA, a secondary bile acid). DCA is more hepatotoxic than CA.[21] Individuals with liver and intestinal diseases show a significantly increase in the concentration of CA and DCA.[22] Therefore, they are often used as a biomarker for the clinical diagnosis of liver and intestinal diseases.[23] Chromatography–mass spectrometry[24,25] and electrochemical methods[26,27] are commonly used for the detection of bile acids. However, these methods are time-consuming and require expensive instruments. For the clinical diagnosis of liver and intestinal diseases, it is highly desirable to develop simple and low-cost sensing platforms for the real-time detection of bile acids.

In our experiments, a 5CB droplet-embedded CHI hydrogel sheet was placed on the bottom of a small glass dish with 60 μL aqueous solution at pH 7.4. Figure 3a–f shows the time-course polarizing microscopy images of the 5CB droplets embedded in the hydrogel sheet after the addition of 200 μM DCA in aqueous solution. Initially, the embedded 5CB droplets show a radial director configuration with a single defect point at the center of the droplets (Figure 3a). The defect point shifts away from the center over time (Figure 3b–d), leading to a preradial director configuration. Finally, the director configuration of the embedded 5CB droplets turns bipolar with two defect points at the poles of the droplets (Figure 3e,f). The radial-to-bipolar transition of the embedded 5CB droplets is a result of the competitive adsorption of the DCA at the surface of the droplets. It is known that bile acids are facial amphiphilic molecules that are extremely surface active. They are able to displace other surface active molecules from the oil–water interface through the competitive adsorption.[28] The surface anchoring energy of the 5CB inside the droplets embedded in the CHI hydrogel films depends on the packing density of the $SC_{14}S$ at the surface of the droplets. The observed radial-to-bipolar transition of the embedded 5CB droplets after the addition of DCA (Figure 3) indicates that the CHI hydrogel matrix is permeable for DCA. The competitive adsorption of the penetrated DCA disrupts/displaces the $SC_{14}S$ from the surface of the embedded 5CB droplets, inducing the radial-to-bipolar configuration transition.

We find that the response time of the 5CB-embedded hydrogel sheet for DCA is 30 s when the concentration of DCA in aqueous solution is in the range from 400 to 100 μM, followed by the sharp increase from 30 s to 6.2 min when the concentration of DCA is reduced from 100 to 10 μM (Figure 3g). The concentration dependence of the response time of the 5CB-embedded hydrogel sheet is also observed for CA (Figure 3g). However, the response time for CA is much longer than that for DCA. For example, the response time of the 5CB droplet-embedded hydrogel sheet is 30 s for DCA and 4 min

DOI: 10.1021/acsami.5b11076
ACS Appl. Mater. Interfaces 2016, 8, 3928–3932

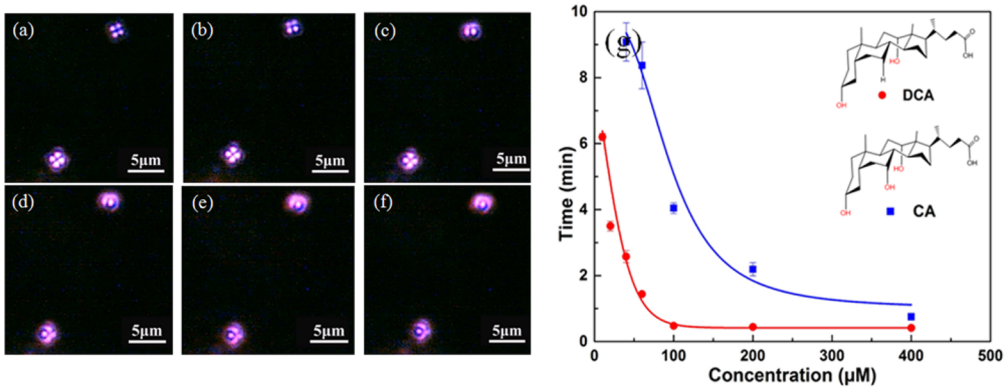

Figure 3. (a–f) Polarizing optical microscopy images of 5CB droplet-embedded CHI hydrogel sheets taken at 0 s (a), 8 s (b), 12 s (c), 17 s (d), 20 s (e), and 23 s (f) after the addition of 200 μM DCA. (g) The response time of the embedded 5CB droplets as a function of DCA and CA concentrations, respectively. The chemical structures of DCA and CA were inset in part g. The data shown in part g were obtained from five sheets for each concentration.

for CA at the same concentration of 100 μM. There is no configuration transition of the embedded 5CB droplets observed for prolonged time periods if the concentration of DCA is lower than 10 μM. As can be seen in Figure 4a that the

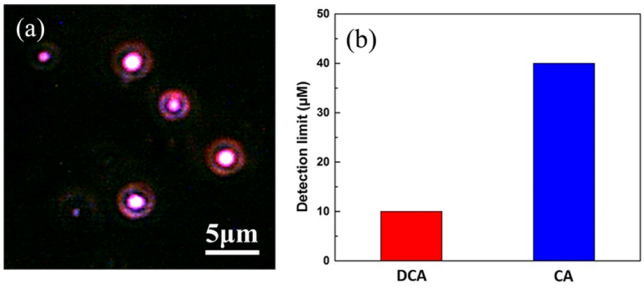

Figure 4. (a) Polarizing optical microscopy images of 5CB droplet-embedded CHI hydrogel sheets after the addition of 10 μM DCA. (b) Detection limit of DCA and CA.

5CB droplets embedded in CHI hydrogel sheets change to bipolar when the DCA concentration reaches 10 μM (defined as a detection limit). The detection limit of the 5CB-embedded hydrogel sheet for CA is 40 μM, which is four times higher than that for DCA (Figure 4b). These results suggest that 5CB droplet-embedded hydrogel sheets are more sensitive for DCA, compared to CA. The pK_a is 6.2 for DCA and 5.2 for CA, respectively. At pH 7.4, both DCA and CA are negatively charged. The critical micelle concentration (CMC) is 10 mM for DCA and 13 mM for CA, respectively.[28] The concentration of CA and DCA used in our experiments is lower than their CMCs. Although DCA and CA share a common steroid backbone, the number of the hydroxyl groups at their steroid backbone is different (see the inset in Figure 3g). It has been shown that the hydrophobicity of DCA bearing two hydroxyl groups is higher than that of CA bearing three hydroxyl groups.[28] The more hydrophobic DCA should be more effective in disrupting/displacing the $SC_{14}S$ from the surface of the embedded 5CB droplets. This may explain why the 5CB droplet-embedded hydrogel sheets show shorter response time and lower detection limit for DCA, compared to CA.

Ascorbic acid (AA) and uric acid (UA), which coexist with bile acids in biological fluids, are major interference species for the detection of bile acids.[29] However, we find that 5CB droplet-embedded hydrogel sheets are insensitive to both AA and UA. There is no configuration transition of the embedded 5CB droplets observed after the addition of 1 mM AA or 1 mM UA in aqueous solution (Figure 5). The selectivity of 5CB

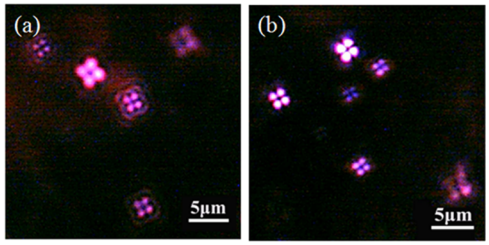

Figure 5. Polarizing optical microscopy images of 5CB droplet-embedded CHI hydrogel sheets after the addition of (a) 1 mM AA and (b) 1 mM UA.

droplet-embedded hydrogel sheets for bile acids over AA and UA should associate with their different amphiphilic nature. Due to lacking amphiphilic nature, AA and UA are unable to disrupt the $SC_{14}S$ packing at the surface of the embedded 5CB droplets.

4. CONCLUSION

We report the formation of 5CB droplet-embedded CHI hydrogel films by the Ag^+ ion-triggered fast gelation of the CHI/$SC_{14}S$ stabilized 5CB emulsion casted on substrates. The sheets cut from the 5CB droplet-embedded hydrogel films can serve as a portable and label-free sensing platform for the detection of bile acids without needing complex detection systems for signal transitions. Unlike CHI/$SC_{14}S$ complex-stabilized 5CB emulsions, the 5CB droplet-embedded hydrogel sheets are easily handed and more stable, allowing the real-time and selective detection of bile acids. We find that the response time and detection limit of 5CB droplet-embedded hydrogel sheets for bile acids relate to their hydrophobicities. The low cost, portability, and simplicity of LC droplet-embedded hydrogel films are highly desirable for the "point-of-care" analysis of bile acids.

AUTHOR INFORMATION

Corresponding Author

*E-mail: Jiyu.Fang@ucf.edu.

DOI: 10.1021/acsami.5b11076
ACS Appl. Mater. Interfaces 2016, 8, 3928–3932

Notes

The authors declare no competing financial interest.

■ ACKNOWLEDGMENTS

This work was supported by the US National Science Foundation (CBET-1264355). The authors thank Prof. Quanfang Chen for his assistance in tensile testings.

■ REFERENCES

(1) Miller, D. S.; Wang, X.; Abbott, N. L. Design of Functional Materials Based on Liquid Crystalline Droplets. *Chem. Mater.* **2014**, *26*, 496−506.
(2) Wang, D.; Park, S. Y.; Kang, I.-K. Liquid Crystals: Emerging Materials for Use in Real-Time Detection Applications. *J. Mater. Chem. C* **2015**, *3*, 9038−9047.
(3) Gennes, P. G. D.; Prost, J. *The Physics of Liquid Crystals*; Clarendon Press: Oxford, 1993.
(4) Tjipto, E.; Cadwell, K. D.; Quinn, J. F.; Johnston, A. P. R.; Caruso, F.; Abbott, N. L. Tailoring the Interfaces between Nematic Liquid Crystal Emulsions and Aqueous Phases via Layer-by-Layer Assembly. *Nano Lett.* **2006**, *6*, 2243−2248.
(5) Sivakumar, S.; Wark, K. L.; Gupta, J. K.; Abbott, N. L.; Caruso, F. Liquid Crystal Emulsions as the Basis of Biological Sensors for the Optical Detection of Bacteria and Viruses. *Adv. Funct. Mater.* **2009**, *19*, 2260−2265.
(6) Zou, J.; Bera, T.; Davis, A. A.; Liang, W.; Fang, J. Y. Director Configuration Transitions of Polyelectrolyte Coated Liquid-Crystal Droplets. *J. Phys. Chem. B* **2011**, *115*, 8970−8974.
(7) Aliño, V. J.; Pang, J.; Yang, K.-L. Liquid Crystal Droplets as a Hosting and Sensing Platform for Developing Immunoassays. *Langmuir* **2011**, *27*, 11784−11789.
(8) Khan, W.; Choi, J. H.; Kim, G. M.; Park, S. Y. Microfluidic Formation of pH Responsive 5CB Droplets Decorated with PAA-*b*-LCP. *Lab Chip* **2011**, *11*, 3493−3498.
(9) Bera, T.; Fang, J. Y. Polyelectrolyte-Coated Liquid Crystal Droplets for Detecting Charged Macromolecules. *J. Mater. Chem.* **2012**, *22*, 6807−6812.
(10) Kim, J.; Khan, M.; Park, S. Y. Glucose Sensor Using Liquid-Crystal Droplets Made by Microfluidics. *ACS Appl. Mater. Interfaces* **2013**, *5*, 13135−13139.
(11) Bera, T.; Fang, J. Y. Protein-Induced Configuration Transitions of Polyelectrolyte-Modified Liquid Crystal Droplets. *J. Phys. Chem. B* **2014**, *118*, 4970−4977.
(12) Yoon, S. H.; Gupta, K. C.; Borah, J. S.; Park, S. Y.; Kim, Y. K.; Lee, J. H.; Kang, I. K. Folate Ligand Anchored Liquid Crystal Microdroplets Emulsion for in Vitro Detection of KB Cancer Cells. *Langmuir* **2014**, *30*, 10668−10677.
(13) Bera, T.; Deng, J.; Fang, J. Y. Tailoring the Surface of Liquid Crystal Droplets with Chitosan/Surfactant Complexes for the Selective Detection of Bile Acids in Biological Fluids. *RSC Adv.* **2015**, *5*, 70094−70100.
(14) Manna, U.; Zayas-Gonzalez, Y. M.; Carlton, R. J.; Caruso, F.; Abbott, N. L.; Lynn, D. M. Liquid Crystal Chemical Sensors that Cells Can Wear. *Angew. Chem., Int. Ed.* **2013**, *52*, 14011−14015.
(15) Peppas, N. A.; Hilt, J. Z.; Khademhosseini, A.; Langer, R. Hydrogels in Biology and Medicine: From Molecular Principles to Bionanotechnology. *Adv. Mater.* **2006**, *18*, 1345−1360.
(16) Bhattarai, N.; Gunn, J.; Zhang, M. Chitosan-Based Hydrogels for Controlled, Localized Drug Delivery. *Adv. Drug Delivery Rev.* **2010**, *62*, 83−99.
(17) Sun, Z.; Lv, F.; Cao, L.; Liu, L.; Zhang, Y.; Lu, Z. Multistimuli-Responsive, Moldable Supramolecular Hydrogels Cross-Linked by Ultrafast Complexation of Metal Ions and Biopolymers. *Angew. Chem., Int. Ed.* **2015**, *54*, 7944−7948.
(18) He, D.; Miao, M.; Sitarz, E. E.; Muiznieks, L. D.; Reichheld, S.; Stahl, R. J.; Keeley, F. W.; Parkinson, J. Polymorphisms in the Human Tropoelastin Gene Modify in Vitro Self-Assembly and Mechanical Properties of Elastin-Like Polypeptides. *PLoS One* **2012**, *7*, e46130.
(19) Wheeler, T. S.; Sbravati, N. D.; Janorkar, A. V. Mechanical & Cell Culture Properties of Elastin-Like Polypeptide, Collagen, Bioglass, and Carbon Nanosphere Composites. *Ann. Biomed. Eng.* **2013**, *41*, 2042−2055.
(20) Armstrong, M. J.; Carey, M. The Hydrophobic-Hydrophilic Balance of Bile Salts. Inverse Correlation between Reverse-Phase High Performance Liquid Chromatographic Mobilities and Micellar Cholesterol-Solubilizing Capacities. *J. Lipid Res.* **1982**, *23*, 70−80.
(21) Delzenne, N. M.; Calderon, P. B.; Taper, H. S.; Roberfroid, M. B. Comparative Hepatotoxicity of Cholic Acid, Deoxycholic Acid and Lithocholic Acid in the Rat: in Vivo and in Vitro Studies. *Toxicol. Lett.* **1992**, *61*, 291−304.
(22) Degirolamo, C.; Modica, S.; Palasciano, G.; Moschetta, A. Bile Acids and Colon Cancer: Solving the Puzzle with Nuclear Receptors. *Trends Mol. Med.* **2011**, *17*, 564−572.
(23) Griffiths, W. J.; Sjövall, J. Bile Acids: Analysis in Biological Fluids and Tissues. *J. Lipid Res.* **2010**, *51*, 23−41.
(24) Que, H.; Konse, T.; Baker, A. G.; Novotny, M. V. Analysis of Bile Acids and Their Conjugates by Capillary Electrochromatography/Electrospray Ion Trap Mass Spectrometry. *Anal. Chem.* **2000**, *72*, 2703−2710.
(25) Perwaiz, S.; Tuchweber, B.; Mignault, D.; Gilat, T.; Yousef, I. M. Determination of Bile Acids in Biological Fluids by Liquid Chromatography-Electrospray Tandem Mass Spectrometry. *J. Lipid Res.* **2001**, *42*, 114−119.
(26) Koide, S.; Ito, N.; Karube, I. Development of a Micro-Planar Amperometric Bile Acid Biosensor for Urinalysis. *Biosens. Bioelectron.* **2007**, *22*, 2079−2085.
(27) Bartling, B.; Li, L.; Liu, C. Determination of Total Bile Acid Levels Using a Thick-Film Screen-Printed Ir/C Sensor for the Detection of Liver Disease. *Analyst* **2009**, *134*, 973−979.
(28) Cabral, D. J.; Hamilton, J. A.; Small, D. M. The Ionization Behavior of Bile Acids in Different Aqueous Environments. *J. Lipid Res.* **1986**, *27*, 334−343.
(29) Martinello, F.; da Silva, E. L. Ascorbic Acid Interference in the Measurement of Serum Biochemical Parameters: in Vivo and in Vitro Studies. *Clin. Biochem.* **2006**, *39*, 396−403.

DOI: 10.1021/acsami.5b11076
ACS Appl. Mater. Interfaces 2016, 8, 3928−3932